AIAA 2001-2778

Mean Flow and Noise Measurements In the Purdue Mach-6 Quiet-Flow Ludwieg Tube

Steven P. Schneider and Craig Skoch
Purdue University
West Lafayette, IN 47907-1282

31st AIAA Fluid Dynamics Conference
11–14 June 2001
Anaheim, CA

Mean Flow and Noise Measurements in the Purdue Mach-6 Quiet-Flow Ludwieg Tube

Steven P. Schneider* and Craig Skoch†
School of Aeronautics and Astronautics
Purdue University
West Lafayette, IN 47907-1282

Abstract

Purdue University continues to develop a 9.5-inch Mach-6 Ludwieg tube for quiet-flow operation to high Reynolds number. The aerodynamic and mechanical design were reported earlier, along with the design and testing of several facility subsystems. Here, measurements of the completed nozzle contour are reported, along with preliminary measurements of the tunnel performance. A fast transducer was used to make pitot-pressure measurements of the mean flow and fluctuations on the nozzle centerline. The run time is about 10 seconds. The mean Mach number decreases from about 6.0 at 1 atm. stagnation pressure to about 5.5 at 10 atm. The pitot-pressure fluctuations decrease from about 4% at a stagnation pressure of 1 atm. to about 1% at 10 atm. Problems with the bleed slot flow are suspected to be the cause of the lack of quiet flow; the pressure fluctuations at the geometrical minimum of the bleed slot range from 0.4% at 1 atm. to 0.2% at 10 atm.

Introduction

Hypersonic Laminar-Turbulent Transition

Laminar-turbulent transition in hypersonic boundary layers is important for prediction and control of heat transfer, skin friction, and other boundary layer properties. However, the mechanisms leading to transition are still poorly understood, even in low-noise environments. Applications hindered by this lack of understanding include reusable launch vehicles such as the X-33 [1], high-speed interceptor missiles [2], hypersonic cruise vehicles [3], and ballistic reentry vehicles [4].

Many transition experiments have been carried out in conventional ground-testing facilities over the past 50 years. However, these experiments are contaminated by the high levels of noise that radiate from the turbulent boundary layers normally present on the wind tunnel walls [5]. These noise levels, typically 0.5-1% of the mean, are an order of magnitude larger than those observed in flight [6, 7]. These high noise levels can cause transition to occur an order of magnitude earlier than in flight [5, 7]. In addition, the mechanisms of transition operational in small-disturbance environments can be changed or bypassed altogether in high-noise environments; these changes in the mechanisms change the parametric trends in transition [6].

For example, linear instability theory suggests that the transition Reynolds number on a 5 degree half-angle cone should be 0.7 of that on a flat plate, but noisy tunnel data showed that the cone transition Reynolds number was about twice the flat plate result. Only when quiet tunnel results were obtained was the theory verified [8]. This is critical, since design usually involves consideration of the trend in transition when a parameter is varied. Clearly, transition measurements in conventional ground-test facilities are generally not reliable predictors of flight performance.

Development of Quiet-Flow Wind Tunnels

Only in the last two decades have low-noise supersonic wind tunnels been developed [5, 9]. This development has been difficult, since the test-section wall boundary-layers must be kept laminar in order to avoid high levels of eddy-Mach-wave acoustic radiation from the normally-present turbulent boundary layers. Quiet tunnels typically have fluctuation levels of 0.1% or less; these are sometimes measured as

*Associate Professor. Associate Fellow, AIAA.
†Research Assistant. Student Member, AIAA.

pitot-pressure fluctuations, using fast pressure transducers, and sometimes as static pressure or massflow fluctuations, using hot wires (e.g., Ref. [10]).

A Mach 3.5 tunnel was the first to be successfully developed at NASA Langley [11]. Langley then developed a Mach 6 quiet nozzle, which was used as a starting point for the new Purdue nozzle [12]. Unfortunately, this nozzle was removed from service due to a space conflict. Langley also attempted to develop a Mach 8 quiet tunnel [9]; however, the high temperatures required to reach Mach 8 made this a very difficult and expensive effort, which was ultimately unsuccessful. The old Langley Mach-6 quiet nozzle is now to be put back in service (Steve Wilkinson, private communication, April 2001). Since this will take some time, the new Purdue Mach-6 quiet flow Ludwieg tube may become the only operational hypersonic quiet tunnel in the world.

Background of the Purdue Mach-6 Quiet-Flow Ludwieg Tube

A Mach-4 Ludwieg tube was constructed at Purdue in 1992, using a 4-inch nozzle of conventional design that was obtained surplus from NASA Langley. By early 1994, quiet-flow operation was demonstrated at the low Reynolds number of about 400,000 [10]. Since then, this facility has been used for development of instrumentation and for measurements of instability waves under quiet-flow conditions (e.g., Ref. [13, 14, 15]). However, the low quiet Reynolds number imposes severe limitations; for example, the growth of instability waves under controlled conditions on a cone at angle of attack was only about a factor of 2 [16]. This is far smaller than the factor of $e^9 - e^{11}$ typically observed prior to transition, and small enough to make quantitative comparisons to computations very difficult.

A facility that remains quiet to higher Reynolds numbers was therefore needed. The low operating costs of the Mach-4 tunnel had to be maintained. However, hypersonic operation was needed in order to provide experiments relevant to the hypersonic transition problems described above. Operation at Mach 6 was selected, since this is high enough for the hypersonic 2nd-mode instability to be dominant under cold-wall conditions, and high enough to observe hypersonic roughness-insensitivity effects, yet low enough that the required stagnation temperatures do not add dramatically to cost and difficulty of operation. Reference [17] describes the overall design of the facility, and the detailed aerodynamic design of the quiet-flow nozzle, carried out using the e^N method.

Attached flow should be maintained in the contraction of the nozzle, since the separation bubbles sometimes observed in wind tunnel contractions are generally unsteady, and would transmit noise downstream into the Mach-6 nozzle. Preliminary analyses have suggested that the low-frequency fluctuations present in the Langley Mach-6 quiet nozzle [12] may be caused by such a separation. Therefore, a detailed aerodynamic design of the contraction was also carried out [18]. Reference [18] also supplies a preliminary report on the detailed mechanical design of the nozzle and contraction, which was carried out during 1997-98. This mechanical design is not trivial, since quiet uniform flow requires very tight tolerances on surface contour and finish.

After some initial tests of fabrication procedures, a purchase order for fabrication of the nozzle and contraction was awarded in January 1999. Reference [19] reported on design and testing of some of the component parts, including the driver-tube heating, the as-measured contraction contour, the throat-region mandrel fabrication and polishing experience, and so on. Ref. [19] also reports the results of numerous measurements of the surface roughness of the mandrel and various test pieces. Finally, Ref. [19] reports temperature measurements carried out on the heated driver tube. Ref. [20] reports on the design and fabrication of the support structure, diffuser, and second-throat section (which also serves as the sting support). It also reports experience with final contraction fabrication, and with operation of the vacuum system. Ref. [20] also reports on the contour measurements on the third attempt at throat-mandrel fabrication. Ref. [21] reports on (1) the completion of the upstream portion of the nozzle, including the wall-contour measurements through section 5, (2) the contraction-region heating apparatus, (3) the burst-diaphragm tests, and (4) the bleed-slot suction system.

The present paper reports the remainder of the nozzle-wall contour measurements, along with initial measurements of the mean flow and freestream noise. During Spring 2001, the tunnel was officially named the Boeing/AFOSR Mach-6 Quiet Tunnel.

The Boeing/AFOSR Mach-6 Quiet Tunnel

Quiet facilities require low levels of noise in the inviscid flow entering the nozzle through the throat, and laminar boundary layers on the nozzle walls. These features make the noise level in quiet facilities an order of magnitude lower than in conventional facilities. To reach these low noise levels, conventional blow-down facilities must be extensively mod-

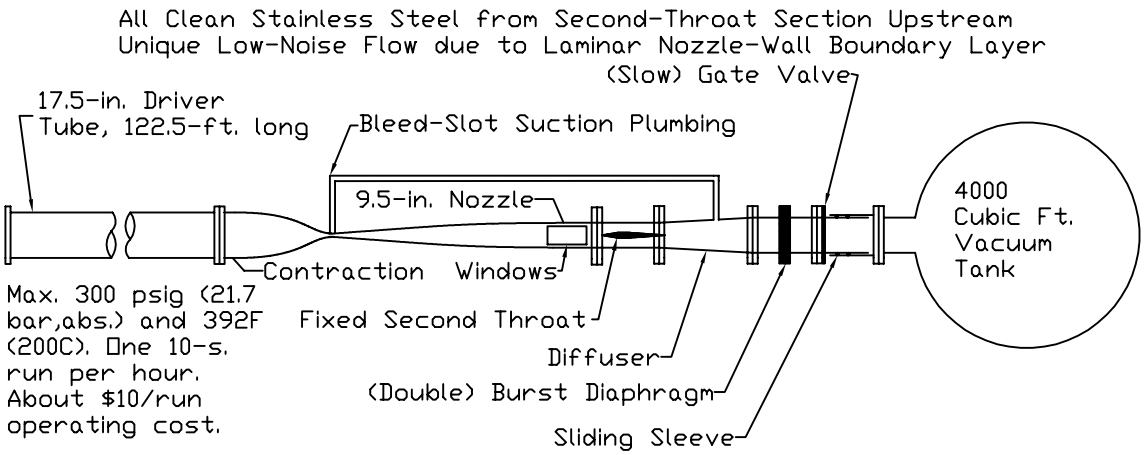

Figure 1: Schematic of Boeing/AFOSR Mach-6 Quiet Tunnel

ified. Requirements include a 1 micron particle filter, a highly polished nozzle with bleed slots for the contraction-wall boundary layer, and a large settling chamber with screens and sintered-mesh plates for noise-reduction [5]. To reach these low noise levels in an affordable way, the Purdue facility has been designed as a Ludwieg tube [10]. A Ludwieg tube is a long pipe with a converging-diverging nozzle on the end, from which flow exits into the nozzle, test section, and second throat (Figure 1). A diaphragm is placed downstream of the test section. When the diaphragm bursts, an expansion wave travels upstream through the test section into the driver tube. Since the flow remains quiet after the wave reflects from the contraction, sufficient vacuum can extend the useful runtime to many cycles of expansion-wave reflection, during which the pressure drops quasi-statically.

Figure 2 shows a portion of the nozzle of the new facility. The region of useful quiet flow lies between the characteristics marking the onset of uniform flow, and the characteristics marking the upstream boundary of acoustic radiation from the onset of turbulence in the nozzle-wall boundary layer. The line A-A' is one estimate of acoustic radiation from an earlier onset of transition on the nozzle wall. A 7.5-deg. sharp cone is also drawn on the figure. The cone is drawn at the largest size for which it is likely to start [22, 23].

Measurements of Nozzle Contour

Maintenance of an accurate nozzle-wall contour is critical to mean flow uniformity, and fabrication with low waviness can be critical to obtaining quiet flow [19]. The nozzle was fabricated in 8 sections, as discussed in Refs. [18] and [19]. Measurements of the contraction contour are presented in Ref. [19], with measurements of the mandrel for the electroformed throat (sec. 1-3) in Ref. [20], and measurements of nozzle sections 4 and 5 in Ref. [21]. The remaining contour measurements are reported here.

Electroformed Throat

The electroformed throat section is shown in Fig. 12 of Ref. [19]. After being electroformed on the mandrel [20], it was removed, and had to be cleaned and polished [21]. It was then shipped to DEI to be fitted to section 4. Although the electroform was expected to duplicate the contour and finish of the mandrel, it was thought desirable to obtain measurements of the actual throat contour, and preliminary tests showed that this could be done without marking the mirror-quality throat finish.

The available data extend only a short length into the throat region, and are shown in Fig. 3. As with the earlier data, measurements were made on the DEI coordinate measuring machine, which has a nominal accuracy of 0.0001 inches. Measurements were made along 4 rays, at 90-deg. azimuthal intervals, at axial intervals of about 0.050 inches. The measurements were therefore made along the x and y axes of the plane transverse to the axial plane. The throat is at $z = 0$ inches; the measurements show a small arbitrary region near the throat, and do not extend all the way to the bleed lip.

Fig. 4 shows the deviations of the measured data from the specified coordinates. On the $+y$ and $-y$ azimuths, the radius is about 0.001 inches too large, over the center section, while on the $+x$ and $-x$ azimuths, the radius is nearly 0.0005 inches too small over the center section. Since Figs. 3 and 4 from Ref. [20] show that the mandrel errors were less than

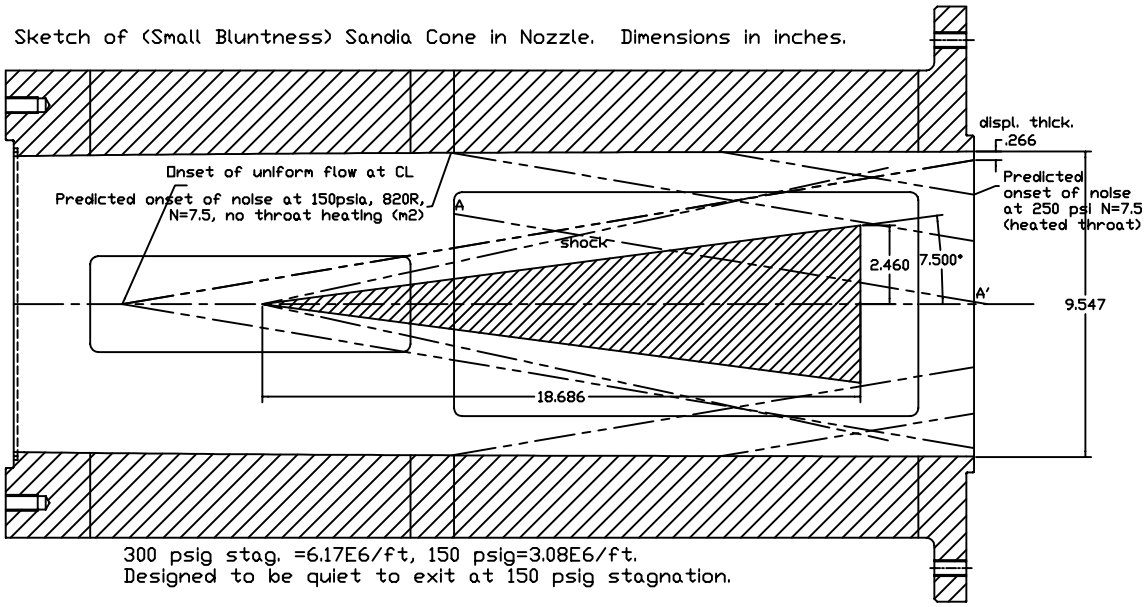

Figure 2: Schematic of Mach-6 Quiet Nozzle with Model

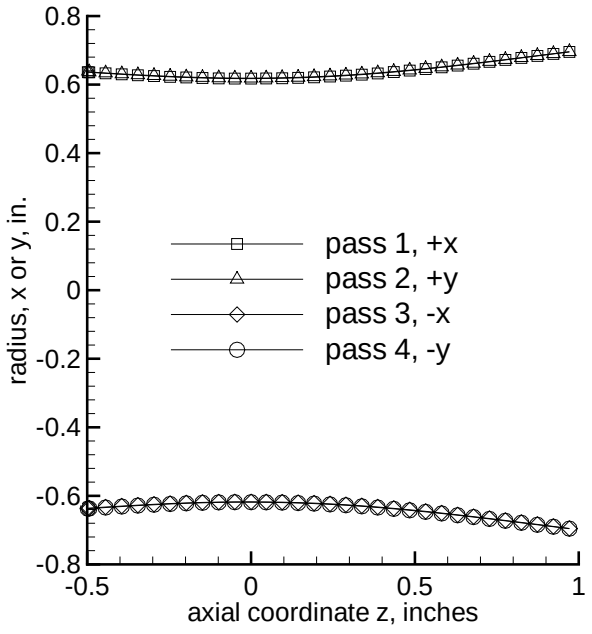

Figure 3: Throat Contour of Electroform

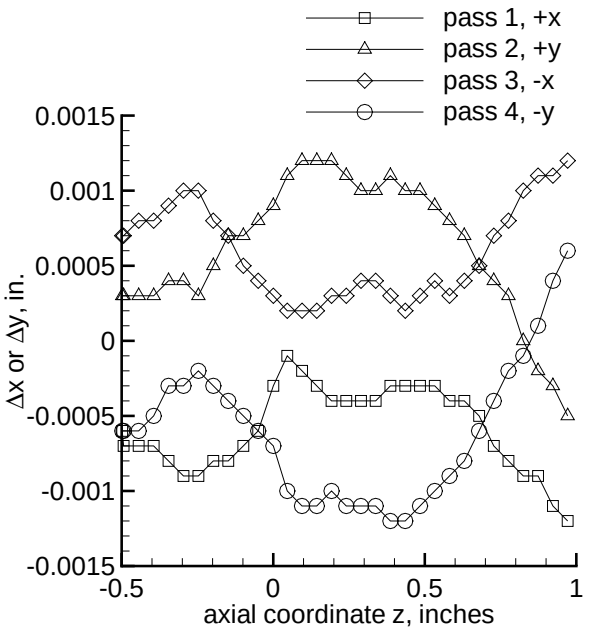

Figure 4: Contour Errors in Throat Region of Electroform

±0.0004 inches in this region, these somewhat larger errors must have occured during electroforming or polishing. The electroform is slightly out of round.

Although the electroforming process is supposed to duplicate the exact contour and finish of the mandrel, it is thought that the electroform distorted slightly during the process, probably due to stress-relieving in the hard nickel layer near the mandrel surface. A small distortion of about 0.0005 inches would explain the discoloration and contamination observed when the mandrel was removed; the cutting and cooling fluids could have worked their way into this small gap during the machining steps. This discoloration was in patches around the azimuth, which would be explained by a nonsymmetric stress relieving. Doug Weber and Larry DeMeno at DEI believed that this problem did not occur with the Langley Mach-6 quiet nozzle, also electroformed by DEI ca. 1990, using only the soft nickel process; this would suggest that stress-relieving in the hard nickel used here near the flow surface caused the slight deformation and accompanying leakage of fluid.

Paul Thomas at Optical Technologies, the polisher, believes that the final polishing/cleaning of the electroform involved the removal of only a few tenths of a mil (ca. 0.0002 inches). The polishing was carried out until visible marks disappeared, and it was believed that the polishing was nearly uniform. The fairly symmetric egg-shaped deviations also suggest that the small non-symmetric deviations are due to the stress-relieving process and not to the polishing.

Joint Between Electroformed Throat and Section 4

After the electroform was completed, it was assembled to section 4, and the joint between the two was smoothed by hand. This hand work was carried out after the final machining of section 4, and after the measurements reported in Ref. [21] were obtained. Because the stainless section 4 is harder than the electroform, section 4 was machined slightly oversize, so a slight amount of material was to be taken from the end of the electroform to smooth out the joint. Unfortunately, the small amount of out-of-round present in the throat of the electroform was also present near the downstream end. The proportion remained about one part in a thousand, so the size of the step was larger.

Fig. 5 shows the measurements taken after completion of the hand work. The end of the electroform is located at $z = 19.26$ inches, and the end of section 4 at $z = 30.265$ in. Fig. 6 shows the deviation of the measured contour from the nominal shape. All of the deviations were computed by DEI using a best-fit

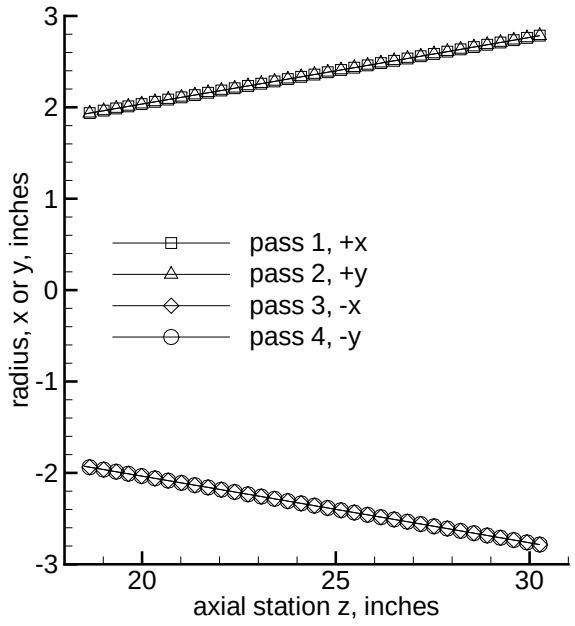

Figure 5: Contour Near Section 4 After Hand Smoothing

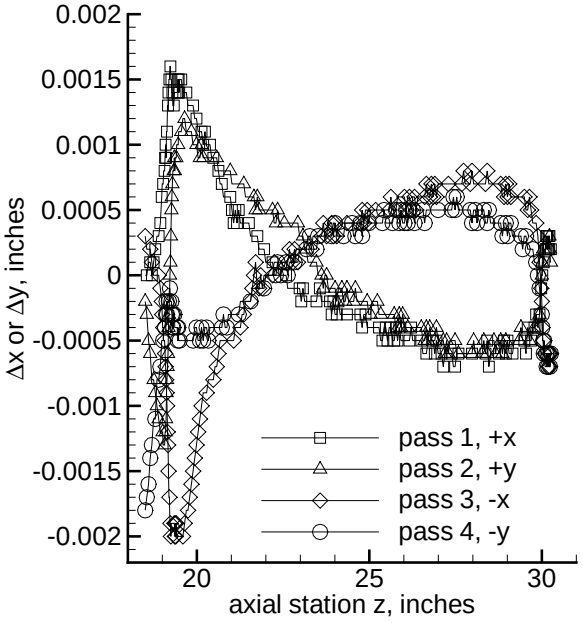

Figure 6: Contour Errors in Section 4 After Smoothing

algorithm to determine the translated location of the ideal shape relative to the measured contour. Thus, repeated measurements on the same shape will give slightly different best-fit deviations. The deviation is within ± 0.001 inches over most of the contour, but becomes larger near the area that was hand smoothed to match the electroform. This region is shown in detail in Fig. 7.

Between $z = 19$ and $z = 20$ in., the radius is too large by about 0.001 to 0.002 in. At $z = 18.5$ inches, the electroform is nearly the correct net size, except along the $-y$ azimuth, where the radius is too large by nearly 0.002 in. There is a wave or near-step of up to about 0.002 in. amplitude, distributed over about 0.25 inches. At $z = 19.265$ in., the roughness criterion of $Re_k = 12$ [19, 17] produces an allowable roughness height of 0.0028 in. at a total pressure of 150 psia, so the wave height falls within the local roughness specification. The local edge Mach number is also large, about 3.9, which would also tend to lessen the effect of this roughness on transition.

Similar steps sometimes occurred during matchup of the other sections, and were removed by honing. However, in this case honing was not thought advisable, due to the differences in the material properties of the nickel and the stainless steel. Since further hand smoothing was not thought likely to improve the contour quality, the shape was accepted as it was.

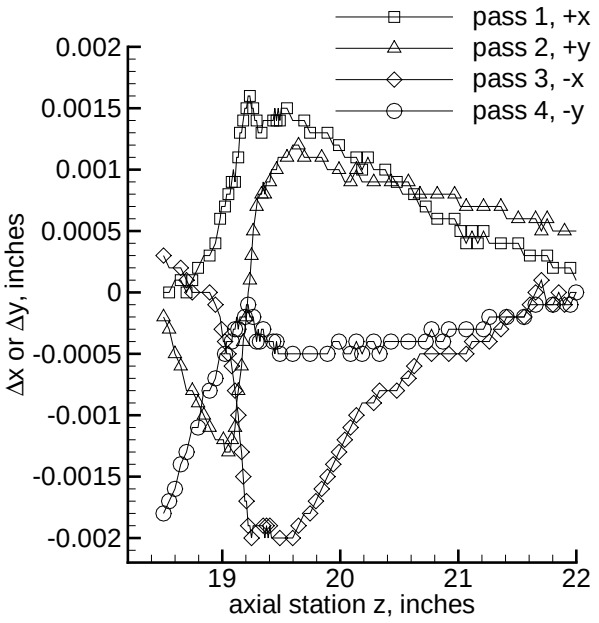

Figure 7: Contour Errors Near Downstream End of Electroform

Section 6

Each section was assembled to the section upstream before performing the final cut. For each section, there is therefore a join line between the first and second machinings. In general, there was a small but detectable wave at this joint; the size was minimized by careful alignment of the part during the second set up in the lathe, after the downstream section was assembled to the earlier parts. This wave was then smoothed out using a 3-stone cylinder hone that was adapted for this purpose by DEI.

Fig. 8 shows the contour of section 6 after the honing. Note that the upstream end of section 5 is at $z = 30.265$, the mechanical joint between sections 5 and 6 is at $z = 42.265$, and the downstream end of section 6 is at $z = 54.265$. The curvature of the contour is visible. The measurements were made along 4 azimuthal rays, as before.

Fig. 9 shows the deviations from the nominal contour. Near the joint at $z = 42.265$, the error becomes slightly larger than the nominal tolerance of ± 0.001 inches. Fig. 10 shows that the slopes, computed by 11-point linear fits to data at 0.050-inch

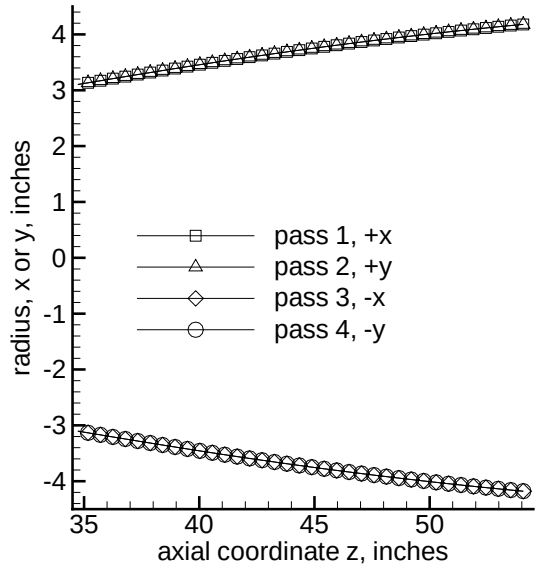

Figure 8: Contour of Section 6 After Honing

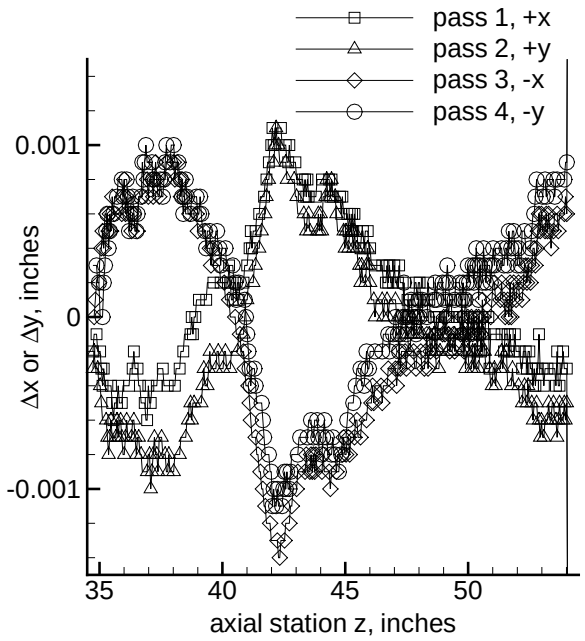

Figure 9: Deviations in Contour of Section 6 After Honing

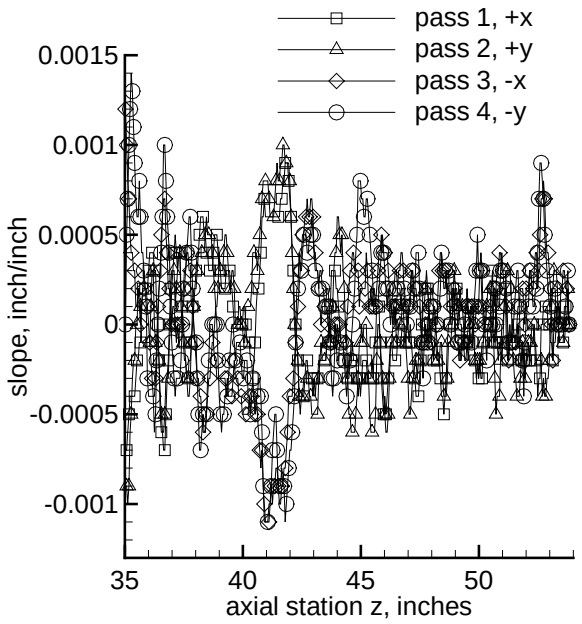

Figure 10: Slopes of Contour Deviation, Section 6 After Honing

intervals, remain within the specification of ± 0.001 inch/inch, except for small regions near $z = 35$ in. and near $z = 42$ in. The largest slopes are within ± 0.0015 in./in. The variable `FLAW` was then computed, as described on p. 8 of Ref. [21]; the value was always less than 0.4×10^{-6} in., after honing, and so was within specification. Before the honing, the slope of the wave at $z = 42$ in. was about 0.004 inch/inch, so the honing was a critical part of the overall process.

Section 7

Fig. 11 shows the contour of section 7 after honing. Section 6 ends at $z = 54.265$ in. and section 7 ends at $z = 71.975$ in. The two sections were separated, measured along azimuthal rays that were carefully aligned, and then the measurements were joined into a composite, shown here. Fig. 12 shows the deviations from nominal. The downstream end of section 7 had a cylindrical flat on it, at this point, for later alignment to section 8, explaining the large deviation at the downstream end. Nearly all of the nozzle is within ± 0.0005 in., except near $z = 54$ in. The 11-point slopes computed for this data remain within ± 0.001 inches, except near $z = 54$ in.

Fig. 13 shows a detail of this region. Recall that the joint is at $z = 54.265$ in. The step at the joint is small, but not negligible. Each side of the joint was measured separately, and the deviations were obtained by separate best-fit analyses, so the step at the joint reflects the errors in the fitting processes as much as the actual step between the sections in any particular assembly. It is difficult to compute slopes automatically in this region, which is the only one with nontrivial waviness. The slopes were thus computed by hand from a figure similar to this one. The largest slope is about 0.0013 inch/inch, and the largest value of `FLAW` is about 1.6×10^{-6} inches. While these measurements are slightly beyond the desired tolerances, they are still very good.

Section 8

Fig. 14 shows the measurements of the contour of the last section, number 8, after final machining and honing. The four azimuthal rays of data, at 90-deg. intervals, run over the middle of the window blanks. Section 8 begins at $z = 71.975$ in., and ends at $z = 101.975$ in. There is no 'test section' downstream of section 8, as all models will be placed in the downstream end of the curved nozzle, where the flow first becomes uniform, and is last affected by the onset of transition in the nozzle-wall boundary layers.

Fig. 15 shows the deviations between the as-machined shape and the nominal specification. Most of the section is within ± 0.0018 in. of nominal, with

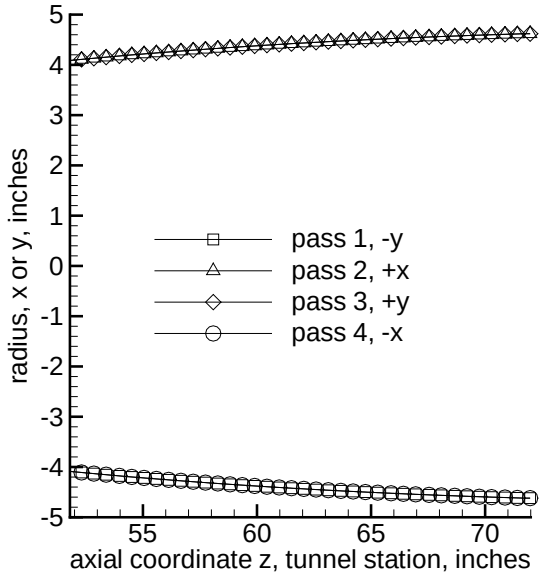

Figure 11: Contour of Section 7 After Honing

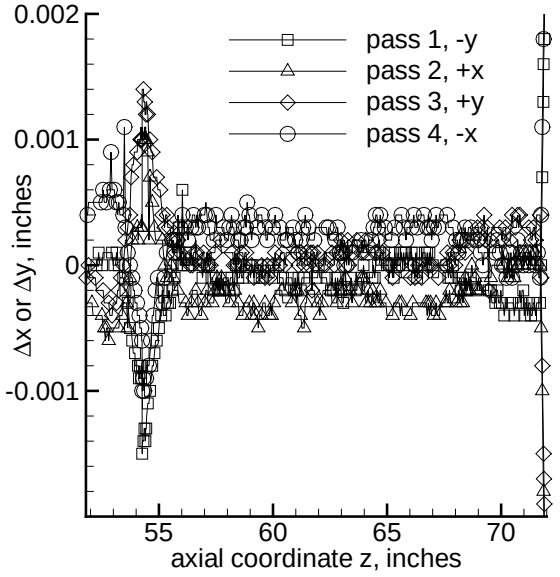

Figure 12: Deviations in Contour of Section 7 After Honing

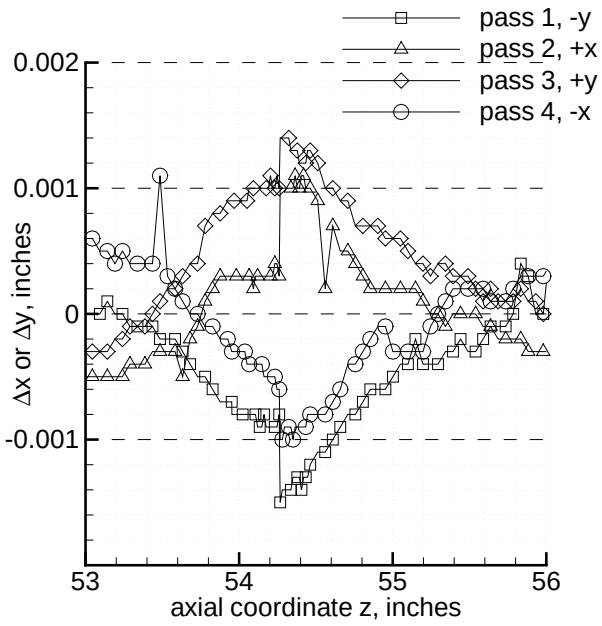

Figure 13: Deviations Near Joint of Sections 6 and 7

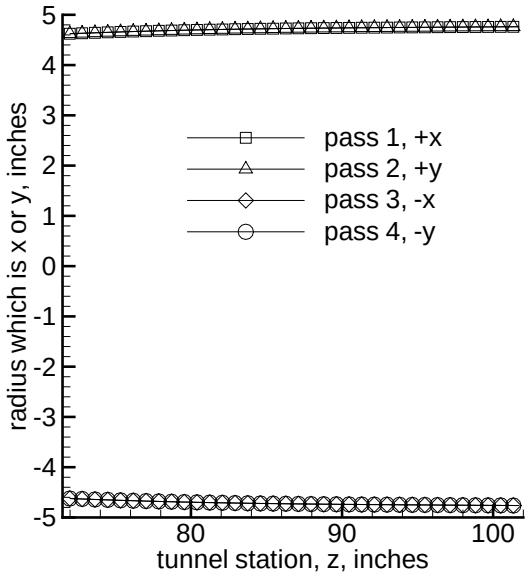

Figure 14: Contour of Section 8 After Honing

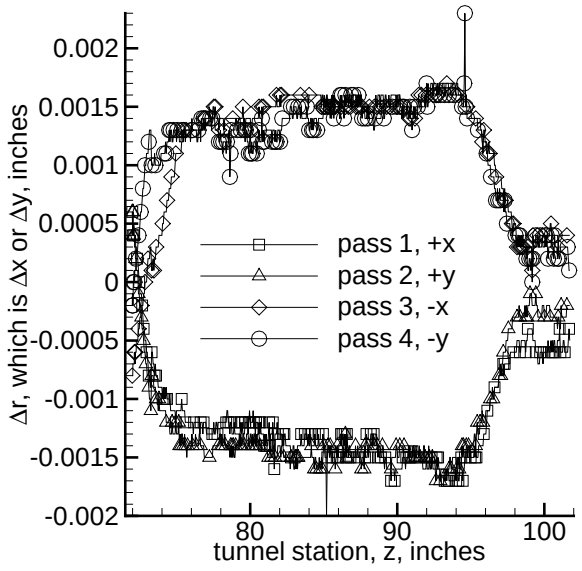

Figure 15: Deviations in Contour of Section 8 After Honing

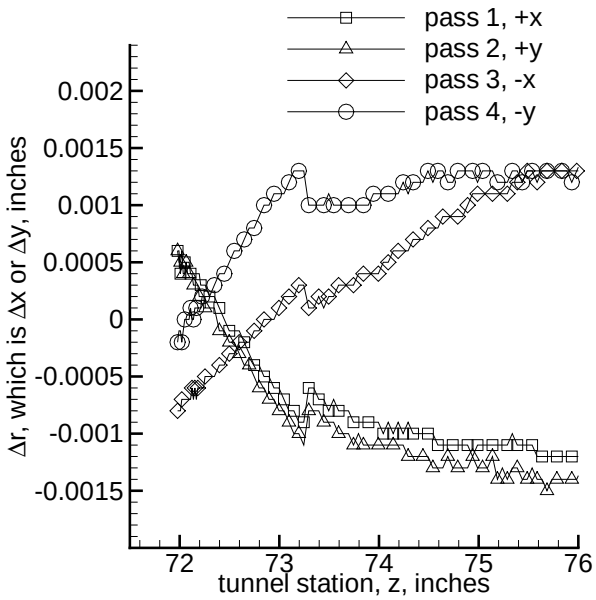

Figure 16: Deviations Near Upstream Window of Section 8

most of it being slightly undersize. A few flier points are evident in the trace; these are believed to be measurements on dust specks. The steps at the window blanks are barely measurable, as is shown in Fig. 16. The four small window blanks in the upstream portion start at about $z = 73.247$ in. and end at about $z = 83.343$ in. The steps at the beginning of the window blanks are less than 0.0005 in. The maximum deviation slopes in the region $72 < z < 74$ are about 0.0013 inch/inch, which is good, although not quite within the original specification. A similar plot at the downstream end of the small blanks shows no detectable flaws.

Fig. 17 shows the deviations in the region of the large and medium window blanks, near the downstream end of the nozzle. These windows start at about $z = 85.072$ in. and end at about $z = 99.198$ in. At the upstream end, no flaws are detectable. Near the downstream end, the joint is just barely detectable, in passes 3 and 4.

The nozzle quality thus appears to be excellent. The joints are barely detectable to the touch, when assembled. The contour accuracy is mostly within ± 0.0015 inches and ± 0.0015 inch/inch. Although this is slightly outside the original specification, it is similar to what was actually obtained on the Langley Mach-8 quiet nozzle (Steve Wilkinson, private communication, 2000). It is probably near the limit

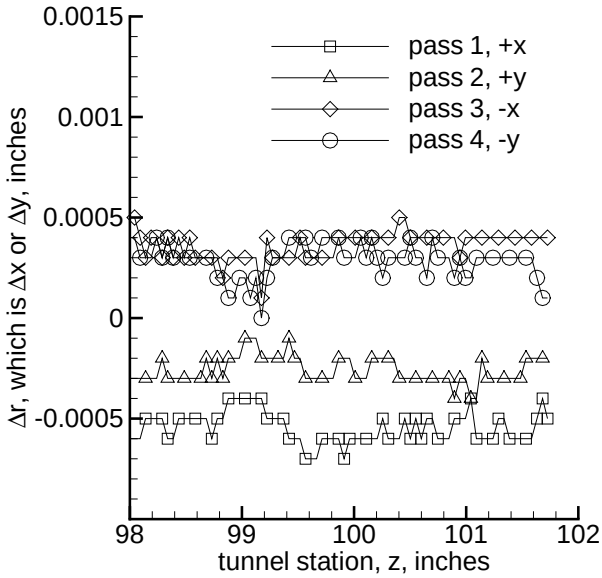

Figure 17: Deviations Near Downstream Window of Section 8

of what is achievable with conventional lathe-cutting processes.

Probe Traversing Mechanism

The traverse is designed to automate motion in the vertical direction. The computer controls have not been set up for this yet, so both the vertical and horizontal movements of the traverse were performed manually. The vertical location was measured internally, and the probe was centered to within 1/16 inch. All measurements have been made with the pitot probe centered vertically. The horizontal movement was both measured internally and externally and is also accurate to about 1/16 inch. More precise control will be provided later when the traverse is completed and the automatic control made operational. A detailed description will be provided in a future paper.

Initial Performance Tests

The first run of the new tunnel was carried out on 19 April 2001. Operations have been fairly smooth, although a few bolts galled in the tapped stainless holes, and had to be replaced. Anti-sieze is now used liberally in all tapped holes, which are in any case outside the sealed flow region. Some difficulty with overheating of the silicone O-ring between contraction sections 1 and 2 was also observed; although the temperature measured on the outside of the contraction was less than 360F, and the silicone O-ring is rated to 450F, the o-ring appeared dried out and stiff when removed upon detection of leakage. Initial experience with cleanliness is good. Although some small dirt spots and grease streaks were evident in the nozzle throat when cleaned after the first few weeks of operation, a second inspection about 2 weeks later revealed almost nothing to clean.

However, the tunnel has been running with noise levels well above the quiet level. Initial measurements have focused on preliminary determination of facility performance, and on determining the cause of the lack of quiet flow. Problems with the bleed-slot flow are the suspected cause of the lack of quiet flow. Since changing the bleed-slot flow requires irreversible machining of small contraction pieces, substantial characterization of the tunnel flow is first to be carried out.

Initial Operating Procedures

Procedures for tunnel operation are now being developed; the following describes those used for most of the runs to date. The driver tube and contraction are heated ahead of time, as these take at least 24 hours to reach equilibrium. Typically, the driver tube and the two downstream sections of the contraction were heated to $170°C$, while the upstream section of the contraction was heated to $160°C$. The upstream section was heated slightly less, because the silicone O-ring in this region showed signs of excessive temperature, suggesting that the actual contraction temperature might have been substantially higher. The thermocouples on the contraction are clamped to the outside of the uninsulated vessel, so they may be reading an artificially low value.

The vacuum pump is turned on and the vacuum tank is pumped down with the gate valve closed (Fig. 1). The diaphragms are inserted and the gate valve is then opened. The driver tube is then filled with air that has been heated by the circulation heater. The circulation heater is turned on to preheat, just before the air begins to flow into the driver tube; the temperature of the circulation heater and the preheat time are additional variables that need to be determined. Typically, the circulation heater was set to $170°C$. For the first run of the day, it was turned on 90 sec. before flow was started; for later runs, it was turned on 30-45 sec. before flow started. This air is allowed to equilibrate for approximately 30 minutes before the run is made (as suggested by the results of Ref. [24]). The electrically-controlled pressure regulator that supplies air to the driver tube is then turned down to zero; little air flows backwards to the regulator from the tube due to a check valve. In all of the runs the initial pressure in the vacuum tank has been below 4 torr. The double diaphragms are burst by bleeding the gap air to vacuum, starting the run.

After the run, the gate valve is closed to allow the vacuum pump to continue pumping down for the next run. After a run the pressure in the driver tube is below atmospheric. It has been observed that the pressure regulator tries to relieve this condition by venting air in from the room, if it is not commanded to put air in from the compressed air tanks. This may be a problem because the room air has not been dried, raising the dewpoint in the driver tube. To prevent this, it is necessary to fill the driver tube with dry air as soon as the gate valve is closed. This concern was not noticed until after most of the runs were done, and this part of the procedure varied. This causes uncertainty regarding the dewpoint of the driver-tube air.

Instrumentation

The mean flow and fluctuations are measured in the nozzle using Kulite XCQ-062-15A fast pressure transducers. These semiconductor diaphragm-type transducers have a diameter of about 0.062 inches. The full-scale pressure range is 0-15 psia; the transducers are mechanically stopped above about 18 psia, so that the calibration remains stable even though the transducers see full stagnation pressures of up to 300 psia before the run starts. These mechanically-stopped transducers are essential to obtaining sufficient signal-to-noise ratio on the small pitot pressures obtained at Mach 6 (about 3% of the stagnation pressure). These transducers are compensated for temperatures to 400F.

A second Kulite is installed in the contraction wall near the geometrical minimum of the bleed slot in the throat. This XCE-062-250A transducer also has a diameter of 0.062 inches, and is compensated for temperatures to 450F. It was installed to allow measurements of the bleed-slot operation; the timing in particular has always been a concern. The full-scale pressure range of this transducer is 250 psia, which keeps it on-scale before the run starts, but makes it less sensitive to small fluctuations.

A third Kulite was later installed to monitor the pressure in the plenum for the throat bleed suction. It replaced two thermocouples, which were initially installed in the downstream end of the contraction, on the upstream face of the suction plenum. This Kulite, a XT-123CE-190-300SG, is rated for 300 psi, sealed gauge, and compensated for temperatures to 350F.

The signals from all three Kulites are obtained using custom electronics. Voltage-reference chips (e.g., REF01) are used to supply 10.00V to the transducers. The output signals are amplified by an INA103 instrumentation amplifier chip, supplying a gain of 100. This output is then high-pass filtered using an RC filter, at about 840Hz, and then amplified by a further factor of 100, to obtain high-resolution measurements of small fluctuations. These Kulite electronics have been used with the Mach-4 Ludwieg tube for several years (cp. Ref. [10]).

The driver-tube temperature is monitored using thermocouples on the outside of the tube, and also using a thermocouple in the air at the upstream end. No cold-wire measurements of the actual gas stagnation temperature have yet been made in the nozzle. The driver-tube pressure before the run starts is measured with a used Heise gauge that was recalibrated to $\pm 0.1\%$ by a NIST-traceable lab. The initial pressure drop due to the expansion wave in the driver tube is very small, due to the very low driver-tube

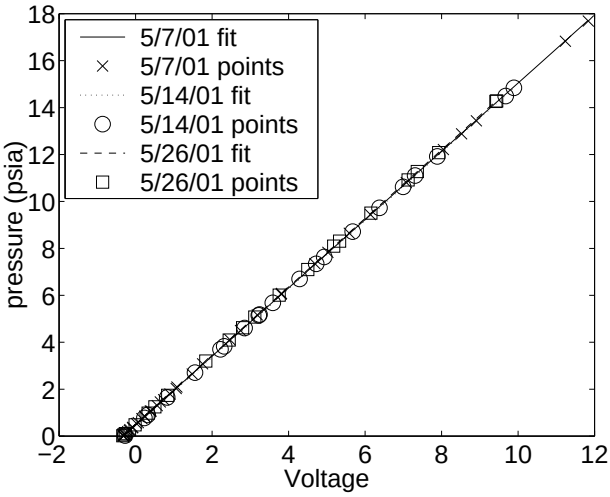

Figure 18: Static Calibrations for Pitot-Pressure Transducer

Mach number of about 0.003; these effects are therefore neglected here.

The Kulite transducers are calibrated using a Paroscientific quartz pressure transducer, which has a specified accuracy of 0.01% over the pressure range of 0 to 30 psia. Above 30 psia, the Heise gauge is used for static calibration. Sample calibrations are shown for the pitot transducer in Fig. 18. Three calibrations were obtained at different times during the acquisition of the data. The three calibrations repeat well, as can be better seen in Fig. 19. The scatter of the points between calibrations is approximately within the scatter of the points around the least-squares linear fit. The rms errors for the three traces are 0.020, 0.014, and 0.011 psi. Since the pitot pressure is about 3% of the total pressure near Mach 6, the error in the pitot pressure should be about 1-2% for total pressures near about 35 psia. A pitot pressure error of about 1% would cause a Mach number error of about 1%, near Mach 6 [25]. Similar calibrations were performed for the throat and plenum transducers. The rms errors for the throat transducer were 0.045, 0.089, and 0.09 psi, while the rms error for the single calibration of the plenum transducer was 0.10 psia.

No meter has yet been installed to measure the driver-gas dewpoint, due to lack of sufficient funds. The operation of the automatically-controlled twin-tower dryer is currently suspect, due to uncertain readings from simple dewpoint monitors containing color-change crystals. Likewise, cold-wire measurements of the driver-tube temperature have not yet been carried out [26], so the true temperature of the

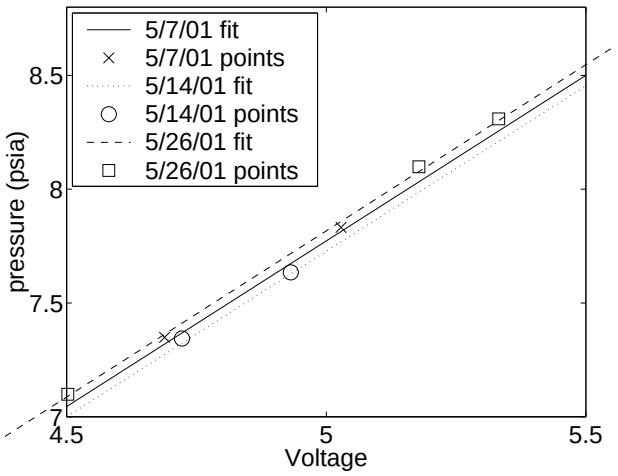

Figure 19: Detail of Static Calibration Data

driver gas in operation remains unknown.

Sample Run Traces

Fig. 20 shows a sample pitot pressure trace, obtained at a driver-tube pressure of 69.89 psia, a driver-tube temperature of 170 deg C, and with the bleed slots open. The initial pressure in the vacuum tank was 3.95 torr. The pitot probe is located at $z = 84.31$ in., about 17.67 in. upstream of the end of the nozzle, and about 9.18 in. downstream of the nominal beginning of uniform flow. Before the run starts, the driver-tube pressure is above the stopped pressure of about 18 psia, so the transducer is pegged. After the run starts, the pressure drops to the supersonic pitot pressure. It then drops further during the run, as air flows out of the driver tube, and the expansion wave undergoes multiple reflections. The supersonic run lasts about 10 sec., which is much more than the 7 sec. anticipated. The long run is thought to be due to better-than-expected pressure recovery in the diffuser.

Fig. 21 shows a detail of the same trace. The pressure drop during the run is about 40%, or about 1% in 0.25 s., although bit noise in the signal is large at this resolution. Fig. 22 shows the AC part of the pitot pressure trace, obtained by reducing the data from AC output of the amplifier. The noise level is about 1.6% of the pitot pressure, which is well above quiet levels, although it would be respectable for a conventional tunnel. Fig. 23 shows a detail of the AC part of the trace. No turbulent spots or other structure is visible in any of the traces obtained so far. The signal appears to be broadband.

Fig. 24 shows the DC signals from the pitot and

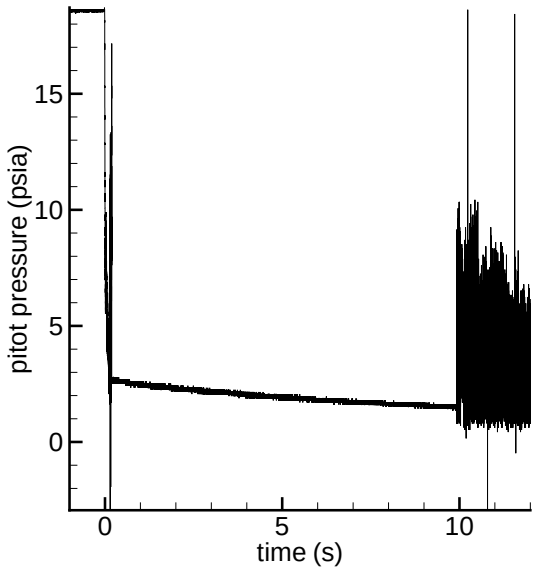

Figure 20: Sample Pitot Pressure Trace

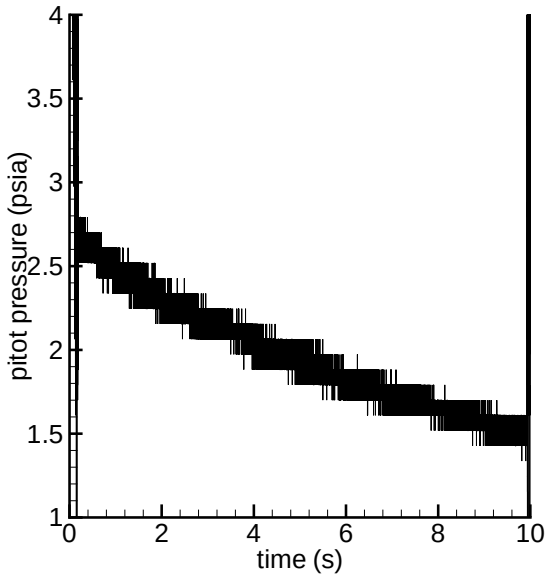

Figure 21: Detail of Sample Pitot Pressure Trace

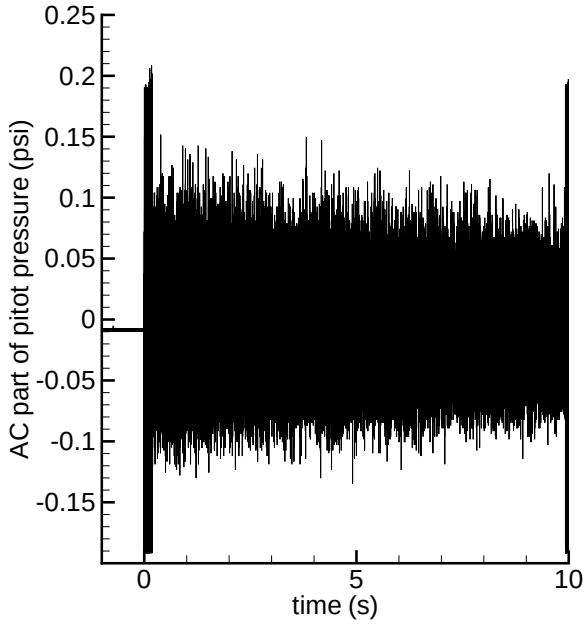

Figure 22: AC Part of Pitot Pressure Trace

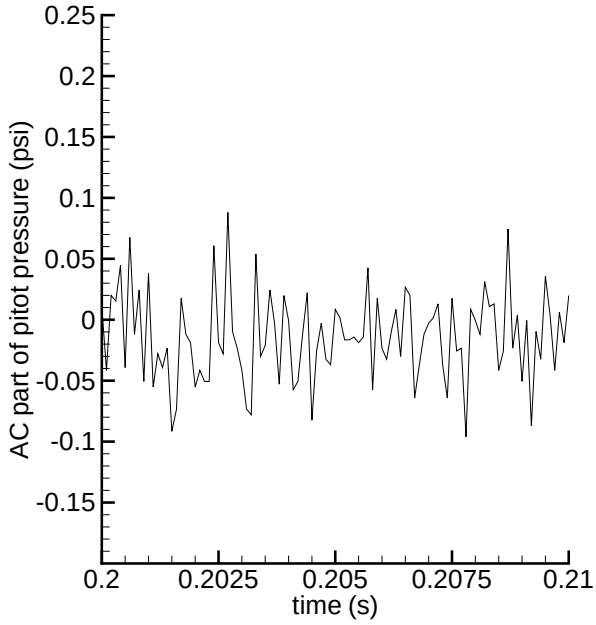

Figure 23: Detail of AC Part of Pitot Pressure Trace

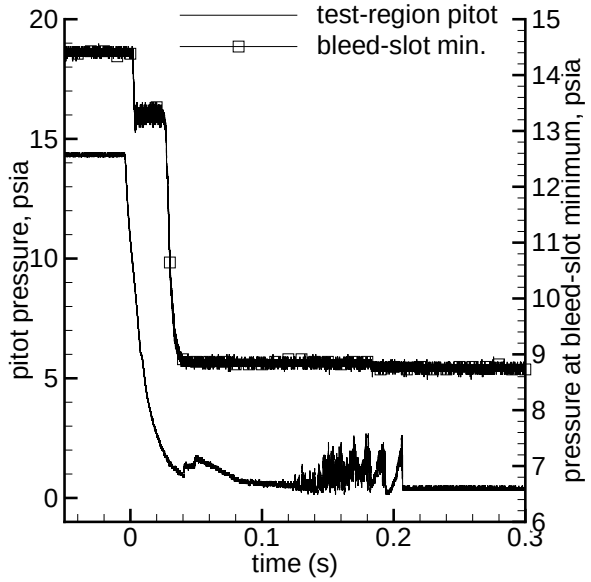

Figure 24: Sample Pitot Pressure Trace During Startup

throat-slot transducers, during the startup process. For this run, the stagnation pressure is 14.37 psia, the stagnation temperature is 170 deg. C, and the bleed slots are open. A run with low stagnation pressure is shown, so that the pitot transducer is not mechanically stopped before the run starts, and there is no delay in picking up the initial pressure drop. The pitot pressure begins to drop at about $t = 0$ sec., where the trigger is set. Due to the longer run of piping to the bleed slots, the pressure at the bleed slot minimum begins to drop about 6 ms later (see the detail in Fig. 25).

Since the pitot transducer is about 6 feet downstream of the throat, it appears that the flow starts through the throat, sucking air back out of the bleed plenum and into the main flow. Then, at about 0.03 sec. in Fig. 25, the expansion wave propagates through the bleed lines and plenum and starts the suction at the bleed throat, dropping the pressure at the bleed minimum to about 9 psia. Since this is about 63% of the driver pressure, or well above the sonic pressure, it may be that the slot flow goes sonic downstream of the minimum. This could be explained by curvature of the sonic line, or by viscous effects. Fig. 24 then shows that the pitot pressure sees a startup flow lasting until about 0.21 s, after which steady hypersonic flow begins.

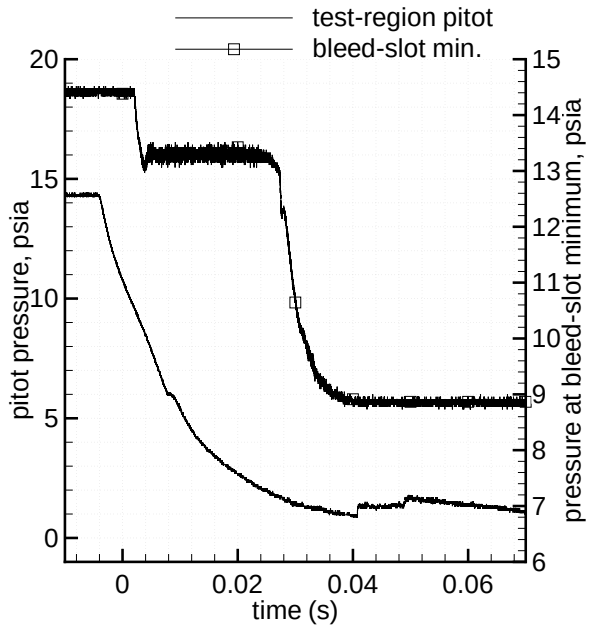

Figure 25: Detailed of Sample Trace During Startup

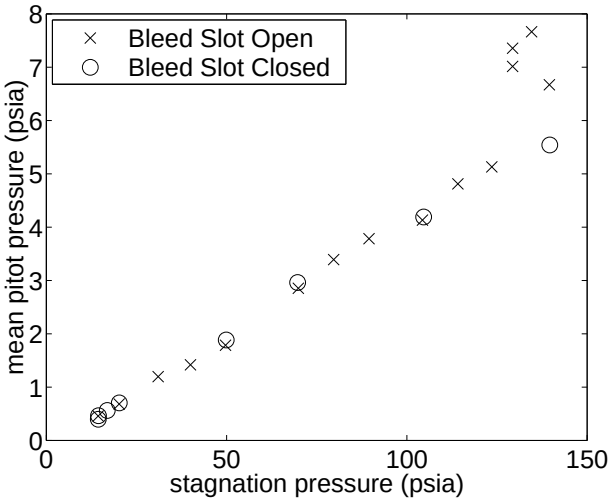

Figure 26: Mean Pitot Pressure at Beginning of Run

Preliminary Tunnel Characterizations

Fig. 26 shows the results of preliminary measurements of the pitot pressure for various initial driver tube pressures. For these runs, the pitot probe is again located at $z = 84.31$ in. The mean pitot pressure is normally obtained from the portion of the record between 0.2 and 0.3 seconds after the run was triggered. The traces were examined visually, and in some cases the average was taken between 0.25 and 0.35 sec., to avoid a longer startup period. There are four points that don't fit within the trend at the high stagnation pressures in figure 26. These points were all taken on the same day, early in the test series, with run conditions similar to all of the other data. These high pitot pressures have not been repeated since these points, and might be the result of a problem with moisture causing a condensation shock.

Fig. 27 shows the resulting Mach numbers, computed using the Rayleigh pitot formula, using the initial driver tube pressure for the stagnation pressure. The initial driver tube pressure is obtained from the pre-run data for the bleed-slot transducer, which agrees with the data recorded from the Heise gauge. For the high pressures near 130 psia, there is a lot of scatter; as discussed before, the scattered runs were all obtained on the same day, and might differ due to condensation effects. Neglecting these runs, the Mach number decreases as stagnation pressure increases up to about 50 psia, and then is nearly constant to 140 psia. The results are nearly independent of whether the bleed valves are open or closed. In earlier Langley measurements in the Mach-6 quiet tunnel, carried out by Frank Chen (Steve Wilkinson, private communication, 15 May 2001), the mean Mach number decreased about 3% when the bleed slots were closed. The change here is much smaller, suggesting that the boundary-layer is turbulent in both cases, and that the spillage of flow over the bleed lip with the slot closed does not greatly change the massflow through the nozzle throat.

The mean Mach number decreases with increasing pressure. This is puzzling, for one would normally expect thinner boundary layers on the nozzle walls at higher pressures, and so a higher Mach number, due to the larger area ratio from the throat. The variation is substantial, and remains to be explained. Transitional effects in the nozzle-wall boundary-layer are one possible cause.

The mean pressure in the geometric minimum of the bleed-slot is shown in Fig. 28. Here, $p_{th,mean}$ is the mean pressure in the bleed-slot throat, and p_0 is the initial driver-tube pressure. It is apparent that the pressure is significantly above the 0.528 value for sonic flow. It thus appears that the transducer is consistently upstream of the sonic line, as discussed above.

The rms pitot fluctuations are shown in Fig. 29. Here, $p_{t2,rms}$ is the rms pitot pressure, and $p_{t2,mean}$ is the mean pitot pressure. The rms is determined by postprocessing the digitized data over the interval from 0.25 to 1.75 sec. after the trigger. The rms pitot pressure decreased from about 4% at 1 atm to-

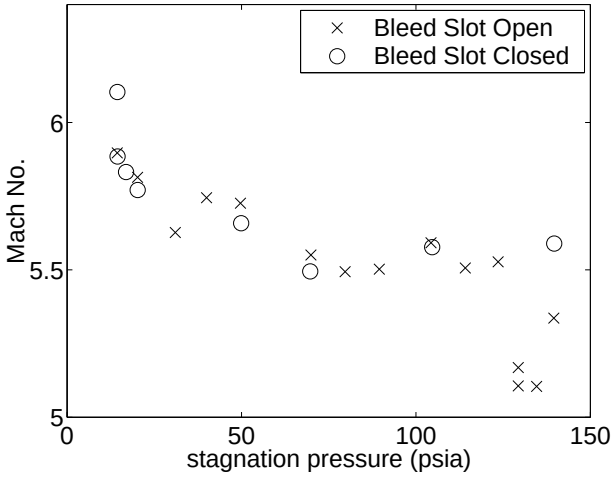

Figure 27: Mean Mach Number vs. Stagnation Pressure

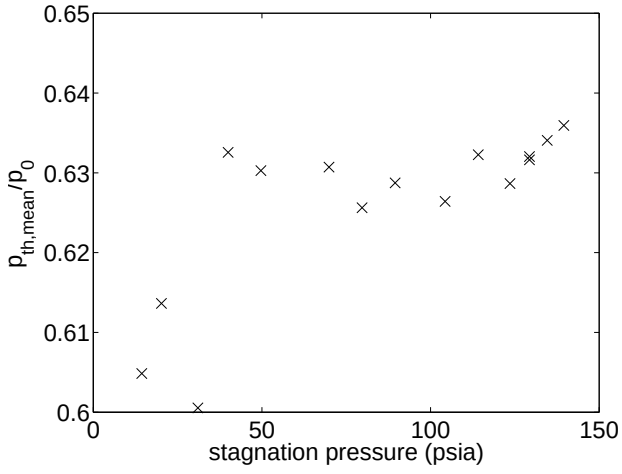

Figure 28: Mean Pressure in Bleed-Slot Throat

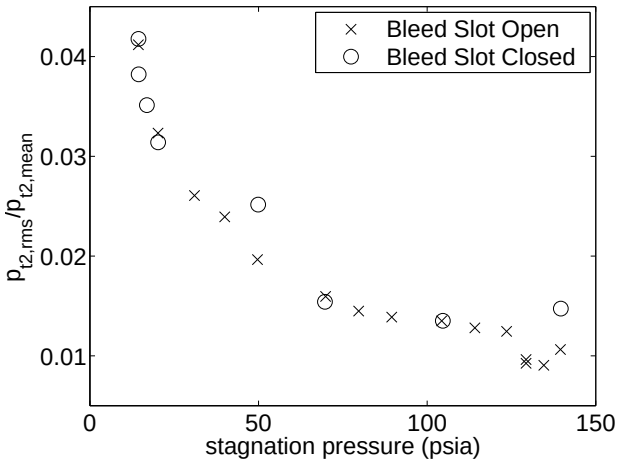

Figure 29: Pitot Pressure Fluctuations vs. Stag. Pressure

tal pressure to about 1% at 140 psia. Since the nominal maximum for quiet flow is about 0.1%, these are not quiet levels. Spectral analysis is presently being carried out.

A few runs with differing conditions produced unexplained results. A run with a cold driver tube and contraction produced substantially lower noise levels that remain unexplained. The driver-tube pressure was 79.0 psia, and the rms pitot pressure was 0.45% of the mean, about 1/3 of the usual value. The Mach number was normal. Longer equilibrating times were also tried, with a hot driver tube, to make sure the driver gas had reached equilibrium. One used a wait of 4 hours, the other with a wait overnight; both used a driver pressure of about 70 psia. These resulted in noise levels similar to the usual runs, but with Mach numbers that were about 5.0, which is about 0.5 lower than similar runs with a 30 minute wait.

The rms fluctuations in the bleed-slot throat pressure ($P_{th,rms}$) are shown in Fig. 30. With the valve open, so that suction air is passing through the slot, the fluctuations decrease about 0.4% at 1 atm. total pressure to about 0.2% at 10 atm. For the sample run at 69.9 psia, the rms throat noise is 0.19% and the electrical noise in the prerun portion of the signal is 0.03%, so the signal/noise ratio is still sufficient to resolve these levels. The noise levels are larger than expected, considering that the mean pressure is above the sonic value (Fig. 28), so that the transducer is located upstream of the sonic point in the slot flow. It should then see only the same level of fluctuation as in the contraction, which should be very low. This suggests that some unsteadiness or separation may be occuring in the bleed slot flow.

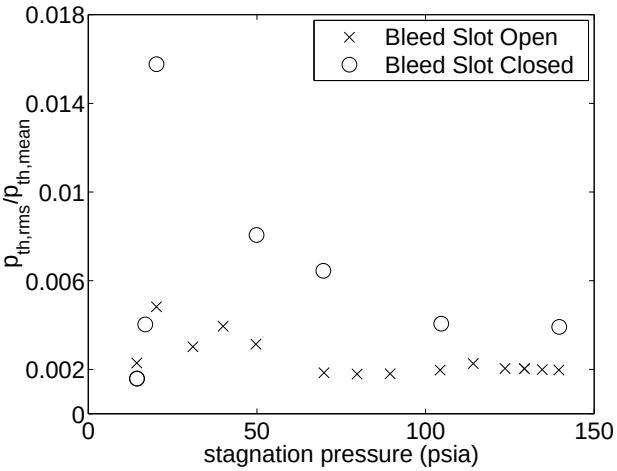

Figure 30: Fluctuations in Bleed-Slot Throat Pressure

Fig. 30 shows an increased noise level in the throat Kulite when the bleed slot is closed, as might be expected, except for the three lowest pressure runs. These low pressure runs produced lower fluctuation levels, for unknown reasons. The lowest pressure run was performed twice at the same conditions with nearly identical results, so that only two low-noise low-pressure points are visible. It should be noted that the lowest pressure run had longer than the usual 30 minutes to reach equilibrium, since it was performed at atmospheric pressure, and the waiting time for the run was only dependent on when the vacuum pressure was sufficiently low. The two next higher pressures, including the run with the highest noise level, only had about 10 minutes to reach equilibrium, due to the difficulty of holding the pressure with the 0.010-inch acetate diaphragms required at those pressures.

Fig. 31 shows what might be happening. If the separating streamline attaches to the bleed lip too far above or below the nosetip, a separation could occur in the flow over the lip. This could cause unsteadiness in the bleed slot flow; any unsteadiness in the bleed flow is likely to feed into the nozzle boundary layer, causing early transition (cp. Ref. [27], where similar but lesser problems are reported).

Initially, there was some concern that the bleed-slot plenum pressure might not be sufficiently low, so that sufficient suction might not be provided through the piping from the diffuser. Fig. 32 shows a time trace of the pressure in the suction slot minimum (P_{th}), along with the pressure in the bleed plenum (P_{pl}). Here, the driver tube stagnation pressure and temperature are 69.95 psia and 170°C, and the initial

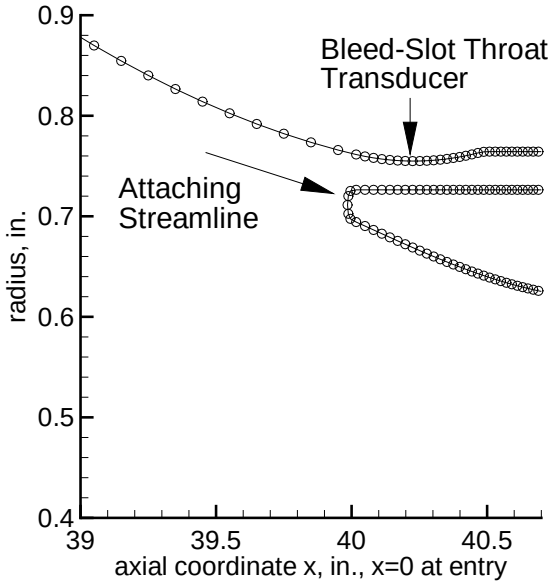

Figure 31: Detail of Bleed-Slot Geometry

vacuum pressure was 0.53 torr. Both pressures start at the initial driver pressure of about 70 psia. The slot throat drops to a constant value when the plenum drops below about 45 psia, and the plenum continues to drop rapidly through the startup time of about 0.2 s. (cp. Fig. 24). At 0.3 s., the plenum pressure is about 5 psia, which is well below the 37 psia needed to establish sonic flow from 70 psia. It appears that the suction piping provides more than enough massflow to establish good suction in the bleed slots.

Preliminary measurements of the mean flow uniformity have also been performed, on the tunnel centerline. Fig. 33 shows the Mach number distribution down the centerline, for a driver pressure of 69.75±0.3 psia and a driver temperature of 170°C. Recall that the nominal onset of uniform flow is at $z = 75.13$ in., and the end of the contoured nozzle is at $z = 101.98$ in. The scatter is about ±2%; the cause of this scatter is unknown. It could be related to dewpoint or calibration problems.

Summary and Future Plans

The new Mach-6 quiet Ludwieg tube has been operational for about 2 months. The mean Mach number on the centerline decreases from about 6.0 at $Re \simeq 3 \times 10^5$/ft. to about 5.5 at $Re \simeq 3 \times 10^6$/ft. The pitot fluctuations decrease from about 4% at the lower Reynolds numbers to about 1% at the higher

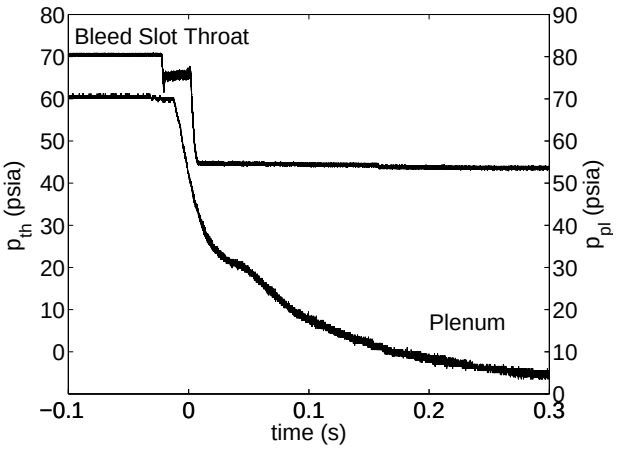

Figure 32: Time Trace Showing Pressure in the Bleed-Slot Plenum

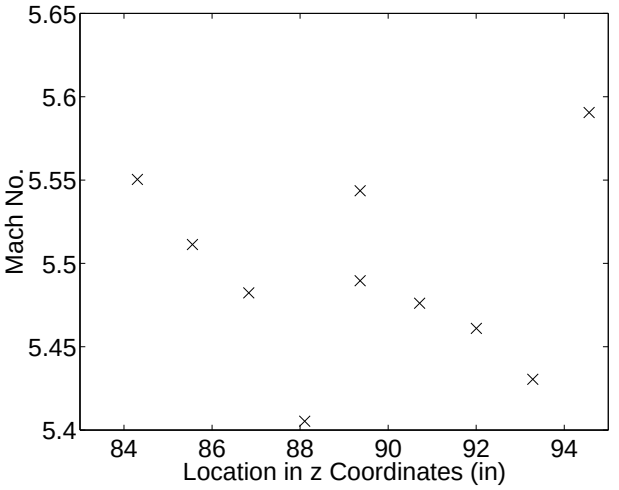

Figure 33: Mach Number Distribution on Tunnel Centerline

ones, so the tunnel is not yet running quiet. Problems with moisture, condensation, and the bleed-slot flow are suspected.

Systematic studies of the driver tube temperature, the contraction temperature, and the temperature and preheat-time of the circulation heater are to be carried out. Cold-wire measurements of the stagnation temperature are to be made in the uniform-flow region. A plexiglas window is to be installed [28], and blockage tests are to be performed with round-cone and slab-delta models. The massflow through the bleed slot is to be varied by machining a throat-ring that forms the geometrical minimum of the slot. The amount of massflow captured by the bleed can also be varied, by machining the last section of the contraction. The temperature of the nozzle throat can be raised to a maximum of about 350F, using equipment already in place. These and other measurements are now to be carried out [29].

Acknowledgements

The research is funded by AFOSR under grant F49620-00-1-0016, monitored by Steve Walker, by Sandia National Laboratory, under contract BG-7114, and by NASA Langley, under Grant NAG1-01-027. Graduate student Shann Rufer assisted with various aspects of the tunnel shakedown and operation. Fabrication of the tunnel was supported primarily by a gift from the Boeing Company and two grants from the Defense University Research Instrumentation Program (F49620-98-1-0284 and F49620-99-1-0278). The first grant was funded by AFOSR, and the second was funded jointly by AFOSR and BMDO. Tunnel fabrication has also been supported by Sandia National Laboratory, and by a gift in memory of K.H. Hobbie. The tunnel design and fabrication has been carried out in cooperation with Dynamic Engineering Inc., of Newport News, Virginia. The generous cooperation of Dr. Steve Wilkinson and the rest of the NASA Langley quiet tunnel group has been critical to our progress.

References

[1] Scott A. Berry, Thomas J. Horvath, Brian R. Hollis, Richard A. Thompson, and H. Harris Hamilton II. X-33 hypersonic boundary layer transition. Paper 99-3560, AIAA, June 1999.

[2] H.A. Korejwo and M.S. Holden. Ground test facilities for aerothermal and aero-optical evalu-

ation of hypersonic interceptors. Paper 92-1074, AIAA, February 1992.

[3] AGARD. *Sustained Hypersonic Flight*, April 1997. CP-600, vol. 3.

[4] Tony C. Lin, Wallis R. Grabowsky, and Kevin E. Yelmgren. The search for optimum configurations for re-entry vehicles. *J. of Spacecraft and Rockets*, 21(2):142–149, March-April 1984.

[5] I.E. Beckwith and C.G. Miller III. Aerothermodynamics and transition in high-speed wind tunnels at NASA Langley. *Annual Review of Fluid Mechanics*, 22:419–439, 1990.

[6] Steven P. Schneider. Effects of high-speed tunnel noise on laminar-turbulent transition. Paper 2000-2205, AIAA, June 2000. Revised version to appear in the J. Spacecraft and Rockets, May-June 2001.

[7] Steven P. Schneider. Flight data for boundary-layer transition at hypersonic and supersonic speeds. *Journal of Spacecraft and Rockets*, 36(1):8–20, 1999.

[8] F.-J. Chen, M.R. Malik, and I.E. Beckwith. Boundary-layer transition on a cone and flat plate at Mach 3.5. *AIAA Journal*, 27(6):687–693, 1989.

[9] S. P. Wilkinson, S. G. Anders, and F.-J. Chen. Status of Langley quiet flow facility developments. Paper 94-2498, AIAA, June 1994.

[10] S. P. Schneider and C. E. Haven. Quiet-flow Ludwieg tube for high-speed transition research. *AIAA Journal*, 33(4):688–693, April 1995.

[11] I. Beckwith, T. Creel, F. Chen, and J. Kendall. Freestream noise and transition measurements on a cone in a Mach-3.5 pilot low-disturbance tunnel. Technical Paper 2180, NASA, 1983.

[12] Alan E. Blanchard, Jason T. Lachowicz, and Stephen P. Wilkinson. NASA Langley Mach 6 quiet wind-tunnel performance. *AIAA Journal*, 35(1):23–28, January 1997.

[13] Steven P. Schneider, Steven H. Collicott, J.D. Schmisseur, Dale Ladoon, Laura A. Randall, Scott E. Munro, and T.R. Salyer. Laminar-turbulent transition research in the Purdue Mach-4 quiet-flow Ludwieg tube. Paper 96-2191, AIAA, June 1996.

[14] J.D. Schmisseur, Steven H. Collicott, and Steven P. Schneider. Laser-generated localized freestream perturbations in supersonic and hypersonic flows. *AIAA Journal*, 38(4):666–671, April 2000.

[15] Terry R. Salyer, Steven H. Collicott, and Steven P. Schneider. Feedback stabilized laser differential interferometry for supersonic blunt body receptivity experiments. Paper 2000-0416, AIAA, January 2000.

[16] Dale W. Ladoon and Steven P. Schneider. Measurements of controlled wave packets at Mach 4 on a cone at angle of attack. Paper 98-0436, AIAA, January 1998.

[17] Steven P. Schneider. Design of a Mach-6 quiet-flow wind-tunnel nozzle using the e**N method for transition estimation. Paper 98-0547, AIAA, January 1998.

[18] Steven P. Schneider. Design and fabrication of a 9-inch Mach-6 quiet-flow Ludwieg tube. Paper 98-2511, AIAA, June 1998.

[19] Steven P. Schneider. Fabrication and testing of the Purdue Mach-6 quiet-flow Ludwieg tube. Paper 2000-0295, AIAA, January 2000.

[20] Steven P. Schneider. Initial shakedown of the Purdue Mach-6 quiet-flow Ludwieg tube. Paper 2000-2592, AIAA, June 2000.

[21] Steven P. Schneider, Shann Rufer, Laura Randall, and Craig Skoch. Shakedown of the Purdue Mach-6 quiet-flow Ludwieg tube. Paper 2001-0457, AIAA, January 2001.

[22] D.A. Bountin, A.N. Shiplyuk, and A.A. Sidorenko. Experimental investigations of disturbance development in the hypersonic boundary layer on a conical models. In H. Fasel and W. Saric, editors, *Laminar-Turbulent Transition. Proceedings of the IUTAM Symposium, Sedona, 1999*, pages 475–480, Berlin, 2000. Springer-Verlag.

[23] C.J. Schueler. An investigation of model blockage for wind tunnels at Mach numbers 1.5 to 19.5. Technical Report AEDC-TN-59-165, Arnold Engineering Development Center, February 1960. DTIC citation AD-232492. Limited distribution.

[24] Scott Edward Munro. Effects of elevated driver-tube temperature on the extent of quiet flow

in the Purdue Ludwieg tube. Master's thesis, School of Aeronautics and Astronautics, Purdue University, December 1996. Available from the Defense Technical Information Center as AD-A315654.

[25] Ames Research Staff. Equations, tables, and charts for compressible flow. Technical Report Report 1135, National Advisory Committee for Aeronautics, 1952.

[26] Steven P. Schneider and Scott E. Munro. Effect of heating on quiet flow in a Mach 4 Ludwieg tube. *AIAA Journal*, 36(5):872–873, May 1998.

[27] J.B. Anders, P.C. Stainback, L.R. Keefe, and I.E. Beckwith. Fluctuating disturbances in a Mach-5 wind tunnel. Paper, AIAA, 1976. In the Proceedings of the 9th Aerodynamic Testing Conference, pp. 185-197.

[28] S.W. Kwon and Steven P. Schneider. Stress analysis for the window of the Purdue Mach-6 quiet-flow Ludwieg tube. Paper 2002-XXXX, AIAA, January 2002. Submitted to the Jan. 2002 AIAA Aerospace Sciences Meeting.

[29] Steven P. Schneider, Craig Skoch, Shann Rufer, and Shin Matsumura. Transition research in the Boeing/AFOSR Mach-6 quiet tunnel. Paper 2002-XXXX, AIAA, January 2002. Submitted to the Jan. 2002 AIAA Aerospace Sciences Meeting.